Optical binding in white light

Shai Maayani, Leopoldo L. Martin, and Tal Carmon*

Technion-Israel Institute of Technology, 3200003 Haifa, Israel
**Corresponding author: tcarmon@technion.ac.il*

Received January 5, 2015; revised March 19, 2015; accepted March 23, 2015;
posted March 24, 2015 (Doc. ID 231466); published April 13, 2015

We experimentally demonstrate, for the first time, binding of aerosols of various sizes and shapes in white light. The optomechancial interaction between particles is long range and is in the underdamped regime. Incoherency allows mitigation of interference fringes to enable monotonically changing the distance between particles from 60 μm to contact, constituting a parametrically controlled testbed for transition studies at new scales. © 2015 Optical Society of America

OCIS codes: (220.4880) Optomechanics; (350.4855) Optical tweezers or optical manipulation.
http://dx.doi.org/10.1364/OL.40.001818

Optical binding is defined as the phenomena occurring when multiple particles are confined in the same optical trap [1,2]. Such multi-particle optical traps were pioneered in aquatic overdamped environments while confined to 2 dimensions [3]. Particles binding in air were then shown with counter-propagating beams [4–6] where particles clung to interference fringes [5] along the direction of propagation. Extension of a 3D tweezer to contain many-bodies [7] was supported by using multi-minimum traps [8–12]. Still, the binding of particles in a single 3D optical trap was studied only theoretically [1].

While atom traps [13–16] are well investigated, extending an optical trap to contain many aerosols levitating in air was not established. Besides the fundamental interest in broadening light–matter interactions to the many-body mesoscopic regime, particle binding will enable, with sufficiently large particle numbers, studies in organization [17] and phase transition [18] as well as measurements of critical slowing down [19]. These experiments will benefit from sensitivity similar to that needed for measuring forces between single molecules [20,21] and for measuring Brownian motion [22]. In addition, particles in such traps can benefit from low dissipation that was suggested to allow access to the quantum-mechanical ground-state at room temperature [23].

Optical tweezers of coherent light were studied in a variety of traps including vortices [24] (for nanoparticles), morphing beams [25], and speckles [26]. Contrary to coherent tweezers, here we use white light [27] that represents a most incoherent form of radiation. Surprisingly maybe, we show that despite the mitigation of coherency in our study, a binding phenomenon is still observed with white light [27]. The levitating ensemble represents an incoherent optomechanical system that does not suffer from material loss [23] of mechanical energy that other optomechanical devices [28,29] are exposed to.

Our experimental setup [Fig. 1(a)] includes a vertically aimed white-light beam that is focused using a 0.07-NA aspherical lens. The repetition rate of our source (Fianium WL-SC400-4) is 10^7 times faster than the phenomena investigated here and thus is treated as a continuous wave.

We start our experiment by dehydrating a liquid concentrate of silica spheres on a coverslip. Then, turn over the coverslip onto a glass cuvette and, with a slight tap, release the dried batch into the cuvette. Our white-light trap is located near the cuvette center where some of the falling particles typically bind.

Silica spheres are chosen here for their low absorption that ranges over a broad spectral span; therefore, thermal effects are reduced.

The white-light beam fulfills two tasks: it traps the particles and enables imaging by means of the scattered light emerging from the top and bottom spots of the spheres [30] [Fig. 2(c)]. As an alternative illumination, back light

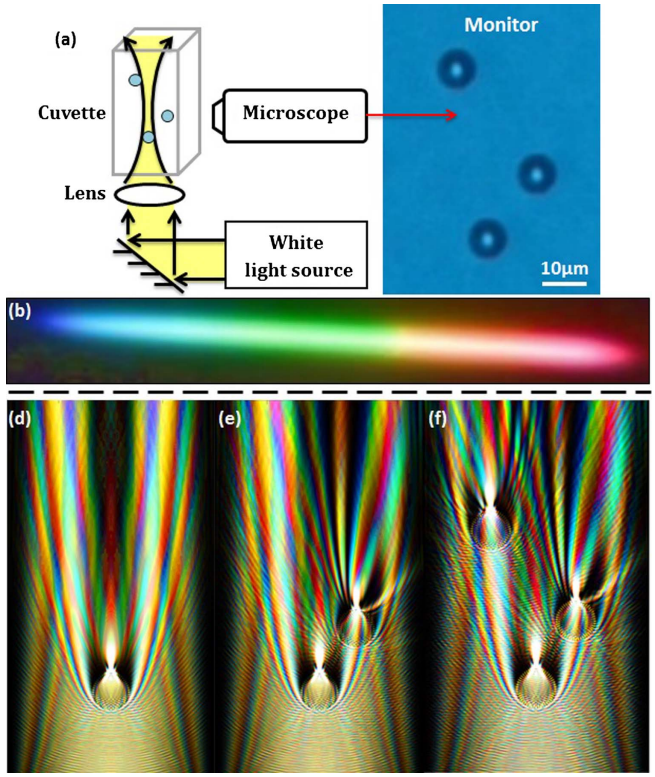

Fig. 1. Experimental setup and simulation. (a) White light is focused to trap multiple spheres near the beam waist. (b) A photograph of our white-light beam after passing through a prism. (d–f) Calculated intensity and color as particles are added reveals that each of the particles gives rise to a new power maximum near the place where the next particle settles. Colors represents the calculated colors at each region and the particles location sites were taken from (b).

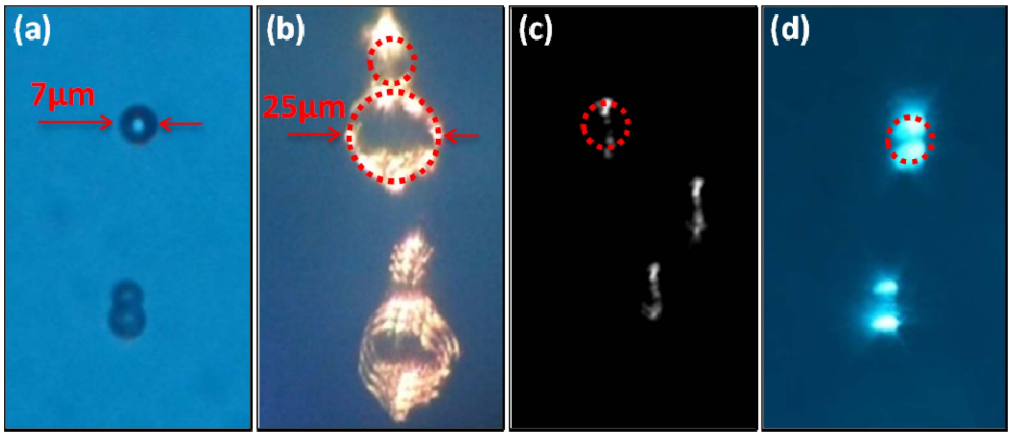

Fig. 2. Experimental results: the system is robust as it can trap 7–25 μm spheres, along with nonspherical particles. The optical power is 6 (a,d), 6.5 (c), and 11 mW (b).

reveals a clearer uniform image of the beads [Fig. 2(a)]. We prefer blue back illumination, with a much lower intensity than that of the trapping beam, for providing better resolution with negligible impact on the trap.

Our major claim of observing aerosol binding is depicted in Fig. 1(b)–1(f) that shows binding of particles near the white-light beam waist. We found trapping versatile among the 7–25 μm spheres that we checked. We observed trapping of spherical as well as of nonspherical aerosols such as a pair of combined identical 7-μm spheres with a single 7-μm sphere [Fig. 2(a) bottom particle] and even binding between two pairs of combined small (7-μm) and large (25-μm) spheres [Fig. 2(b)]. In accordance to these experimental results, white-light binding is applicable to a variety of particles of different sizes and shapes.

As one can see in Fig. 3(a), we measure a linear dependency between the particles' separation and the trapping beam power. Reducing the power monotonically draws the particles closer until they join together [Fig. 3(a) bottom inset]. Yet, increasing the intensity does not separate the particles. By tuning the input power, we can therefore control the gap between particles, a feature that might benefit inspection of inter-particle forces or reactions over short distances. Interestingly, the higher particle sticks to the lower one from its side in accordance with our calculated potential well that will be provided in what follows.

A Fourier transform of the particles' height position versus time reveals a frequency of 2 Hz [Fig. 3(b)] with a linewidth that attests to operation in the underdamped regime [31]. We note that smaller particles at higher power counter-propagating beams are expected to oscillate at rates above kHz.

In order to check how the motion of one body in the ensemble corresponds with the movements of its neighbor, we monitor the height of different particles over a long period of time. As expected, we see that fluctuations of one particle are typically associated with the dynamics of its neighbor as measured in the places marked in red in Fig. 4. Correlation between the particles' fluctuations can be attributed to the fact that the top optical traps are generated from light that is scattered by the bottom trapped particle. Fluctuations in the bottom particle will therefore accordingly affect the upper trap and the particle residing there.

In more detail, a spherical particle functions as a spherical lens that scatters the light so that the initial Gaussian beam is modified. Additionally, multiple reflections between two neighbors link between their motions.

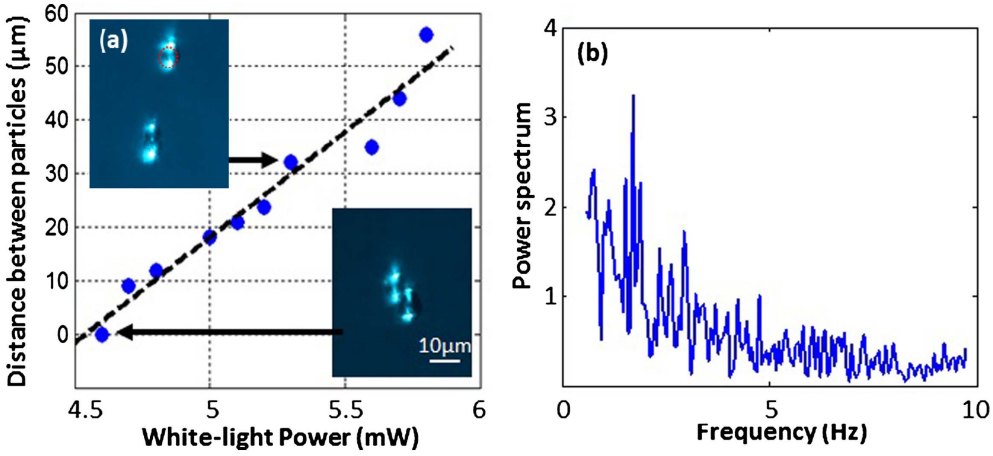

Fig. 3. Experimental results: (a) the spheres are monotonically getting closer to each other as trap power decreases. By the end of this test, the particles were touching each other as seen in the lower inset. (b) The power spectrum of the vertical movement.

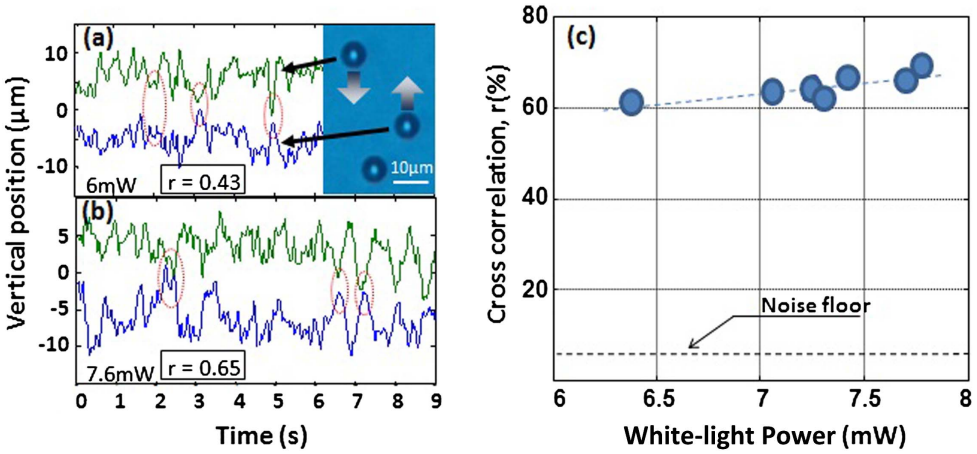

Fig. 4. Experimental results: long-range interaction. Plots (a) and (b) describe the position of two particles as a function of time while trap power increases from 6 to 7.6 mW. One particle affects the motion of the other as seen in the places marked in red and as evident by the cross-correlation constant, r (c) (sign reversed), calculated over a time period of 2 min.

As for interaction between particles, which is mediated by air pressure, it seems that this effect is unlikely. Mainly, because our experimental results shows that the particles move out of phase in contrast with what is expected if motion would have been mediated by air.

To give a sense of scale to the coupling between particles, we measure the cross-correlation, $r = abs\{\langle(X_1-\mu_1)(X_2-\mu_2)/(\sigma_1\sigma_2)\rangle\}$, between the motion of one particle, X1, and the motion of its neighbor in the opposite direction, X2, where μ and σ are the mean value and standard deviation, respectively. The correlation rose from 57% to 74% when the power was increased, as one can see in Fig. 4(b). As a control group, measuring the correlation between two such uncorrelated experiments resulted in a correlation of 5% which is 14 times smaller than in the experiment [Fig. 4(c)]. The interaction between the particles is over a long range of 20 μm, which is equivalent to 20 wavelengths of light or 3 sphere diameters.

In what follows, a simplified 2-dimensional model calculates the scattering structure for a typical experimental configuration using finite-elements frequency domain (COMSOL full-wave solver) in the presence of a Gaussian beam waist. While blue here represents a short wavelength and red-long, part of the power in our experiment was in the infrared so that our plot is not a one-to-one representation of a visual perception. As one can see in Fig. 1(d), the first particle that is trapped by the white-light beam creates a scattering structure with side lobes where the second particle settles [Fig. 1(e)]. Similarly, with the second particle, an intensity maximum is present at the left-hand side [Fig. 1(e)] where the third particle settles [Fig. 1(f)]. The three-particle simulation [Fig. 1(f)] is put just below the corresponding experimental results [Fig. 1(b)] to allow comparison. Contrary to what one might expect with coherent-light, the interference pattern here is with relatively low visibility and of a smooth and colorful character as typical to white light. As expected, the path that the top particle in Fig. 3 took toward the bottom one corresponds with the shape of the side lobe calculated in Fig. 1(d).

In closing, our system experimentally demonstrates binding of particles of various sizes and diverse shapes in white light that is similar to sunlight. While coherent systems with ensembles of atoms are widely studied, our experiments represent an extension of such systems to the new regime of white light and mesoscopic particles.

References

1. J. M. Taylor, *Optical Binding Phenomena: Observations and Mechanisms* (Springer, 2011).
2. K. Dholakia and P. Zemánek, Rev. Mod. Phys. **82**, 1767 (2010).
3. M. M. Burns, J.-M. Fournier, and J. A. Golovchenko, Phys. Rev. Lett. **63**, 1233 (1989).
4. D. M. Gherardi, A. E. Carruthers, T. Čižmár, E. M. Wright, and K. Dholakia, Appl. Phys. Lett. **93**, 041110 (2008).
5. M. Guillon, O. Moine, and B. Stout, Phys. Rev. Lett **96**, 143902 (2006).
6. D. Rudd, C. Lopez-Mariscal, M. Summers, A. Shahvisi, J. GutiÚrrez-Vega, and D. McGloin, Opt. Express **16**, 14550 (2008).
7. D. G. Grier, Nature **424**, 810 (2003).
8. K. Visscher, S. P. Gross, and S. M. Block, IEEE J. Sel. Top. Quantum Electron. **2**, 1066 (1996).
9. V. G. Shvedov, A. S. Desyatnikov, A. V. Rode, W. Krolikowski, and Y. S. Kivshar, Opt. Express **17**, 5743 (2009).
10. T. Čižmár, L. D. Romero, K. Dholakia, and D. Andrews, J. Phys. B **43**, 102001 (2010).
11. M. Frawley, J. M. Ward, and S. Nic Chormaic, *Optical Trapping and Manipulation of Micron-Sized Particles Using a Bright Tapered Optical Fiber* (Optical Society of America, 2010), paper LMB3.
12. C. D. Mellor, T. A. Fennerty, and C. D. Bain, Opt. Express **14**, 10079 (2006).
13. J. T. Barreiro, M. Müller, P. Schindler, D. Nigg, T. Monz, M. Chwalla, M. Hennrich, C. F. Roos, P. Zoller, and R. Blatt, Nature **470**, 486 (2011).
14. J. Gieseler, B. Deutsch, R. Quidant, and L. Novotny, Phys. Rev. Lett. **109**, 103603 (2012).
15. W. D. Phillips, Rev. Mod. Phys. **70**, 721 (1998).
16. D. W. Sesko, T. Walker, and C. E. Wieman, J. Opt. Soc. Am. B **8**, 946 (1991).
17. G. Nicolis and I. Prigogine, *Self-Organization in Nonequilibrium Systems* (Wiley, 1977), pp. 160–212, 339–352.
18. T. Ramakrishnan and M. Yussouff, Phys. Rev. B **19**, 2775 (1979).
19. H. Yahata and M. Suzuki, J. Phys. Soc. Jpn. **27**, 1421 (1969).

20. S. C. Kuo and M. P. Sheetz, Science **260**, 232 (1993).
21. J. T. Finer, R. M. Simmons, and J. A. Spudich, Nature **368**, 113 (1994).
22. T. Li, S. Kheifets, D. Medellin, and M. G. Raizen, Science **328**, 1673 (2010).
23. D. Chang, C. Regal, S. Papp, D. Wilson, J. Ye, O. Painter, H. Kimble, and P. Zoller, Proc. Nat. Acad. Sci. **107**, 1005 (2010).
24. V. G. Shvedov, A. V. Rode, Y. V. Izdebskaya, A. S. Desyatnikov, W. Krolikowski, and Y. S. Kivshar, Phys. Rev. Lett. **105**, 118103 (2010).
25. P. Zhang, J. Prakash, Z. Zhang, M. S. Mills, N. K. Efremidis, D. N. Christodoulides, and Z. Chen, Opt. Lett. **36**, 2883 (2011).
26. V. Shvedov, A. Rode, Y. V. Izdebskaya, D. Leykam, A. Desyatnikov, W. Krolikowski, and Y. S. Kivshar, J. Opt. **12**, 124003 (2010).
27. P. Li, K. Shi, and Z. Liu, Opt. Lett. **30**, 156 (2005).
28. T. Carmon, H. Rokhsari, L. Yang, T. J. Kippenberg, and K. J. Vahala, Phys. Rev. Lett. **94**, 223902 (2005).
29. M. Eichenfield, R. Camacho, J. Chan, K. J. Vahala, and O. Painter, arXiv preprint arXiv:0812.2953 (2008).
30. M. Guillon and B. Stout, Phys. Rev. A **77**, 023806 (2008).
31. R. Di Leonardo, G. Ruocco, J. Leach, M. Padgett, A. Wright, J. Girkin, D. Burnham, and D. McGloin, Phys. Rev. Lett. **99**, 010601 (2007).